Spectral design of temperature-invariant narrow bandpass filters for the mid-infrared

Stolberg-Rohr, Thomine Kirstine; Hawkins, Gary J.

Published in:
Optics Express

Link to article, DOI:
10.1364/OE.23.000580

Publication date:
2015

Document Version
Publisher's PDF, also known as Version of record

Spectral design of temperature-invariant narrow bandpass filters for the mid-infrared

Thomine Stolberg-Rohr[2] Gary J. Hawkins[1,*]

[1]*The University of Reading, Infrared Multilayer Laboratory, School of Systems Engineering,Whiteknights, Reading, Berkshire, RG6 6AY, England, UK*

[2]*Technical University of Denmark (DTU), DTU Chemical Engineering, Søltofts Plads 229, 2800 Kgs. Lyngby, Denmark*

[*]*g.j.hawkins@reading.ac.uk*

Abstract: The ability of narrow bandpass filters to discriminate wavelengths between closely-separated gas absorption lines is crucial in many areas of infrared spectroscopy. As improvements to the sensitivity of infrared detectors enables operation in uncontrolled high-temperature environments, this imposes demands on the explicit bandpass design to provide temperature-invariant behavior. The unique negative temperature coefficient ($dn/dT<0$) of Lead-based (Pb) salts, in combination with dielectric materials enable bandpass filters with exclusive immunity to shifts in wavelength with temperature. This paper presents the results of an investigation into the interdependence between multilayer bandpass design and optical materials together with a review on invariance at elevated temperatures.

OCIS codes: (350.2460) Filters, interference; (300.6340) Spectroscopy, infrared; (310.0310) Thin films; (310.4165) Multilayer design; (310.6188) Spectral properties; (310.6860) Thin films, optical properties.

References and links

1. G. J. Hawkins, R. Hunneman, R. Sherwood, and B. M. Barrett, "Infrared filters and coatings for the High Resolution Dynamics Limb Sounder (6-18 microm)," Appl. Opt. **39**(28), 5221–5230 (2000).
2. T. Katsumata, R. Nishimura, K. Yamaoka, E. G. Camargo, T. Morishita, K. Ueno, S. Tokuo, H. Goto, and N. Kuze, "Uncooled InGaSb photovoltaic infrared detectors for gas sensing," J. Cryst. Growth **378**, 611–613 (2013).
3. A. G. U. Perera, P. V. V. Jayaweera, G. Ariyawansa, S. G. Matsik, K. Tennakone, M. Buchanan, H. C. Liu, X. H. Su, and P. Bhattacharya, "Room temperature nano- and microstructured photon detectors," Microelectron. J. **40**(3), 507–511 (2009).
4. P. V. V. Jayaweera, S. G. Matsik, A. G. U. Perera, H. C. Liu, M. Buchanan, and Z. R. Wasilewski, "Uncooled infrared detectors for 3-5 um and beyond," Appl. Phys. Lett. **93**(2), 021105 (2008).
5. T. Stolberg-Rohr, R. Buchner, S. Clausen, J. M. Jensen, A. Skouboe, G. Hawkins, and R. S. Hansen, "In optics humidity compensation in NDIR exhaust gas measurements of NO2," in *Advanced Photonics Conference*, OSA Technical Digest (online) (Optical Society of America, 2014), paper SeTh1C.3.
6. R. Mark, D. Morand, and S. Waldstein, "Temperature control of the bandpass of an interference filter," Appl. Opt. **9**(10), 2305–2310 (1970).
7. C. S. Evans, R. Hunneman, and J. S. Seeley, "Optical thickness changes in freshly deposited layers of lead telluride," J. Phys. D. **9**(2), 321–328 (1976).
8. J. S. Seeley, R. Hunneman, and A. Whatley, "Temperature-invariant and other narrow band IR filters containing PbTe, 4-20 um," Proc. SPIE **246**, 83–96 (1980).
9. C. R. Pidgeon and S. D. Smith, "Resolving power of multilayer filters in nonparallel light," J. Opt. Soc. Am. **54**(12), 1459–1466 (1964).
10. J. S. Seeley, G. J. Hawkins, and R. Hunneman, "Performance model for cooled IR filters," J. Phys. D **21**(10S), S71–S74 (1988).
11. B. Li, S. Y. Zhang, J. C. Jiang, D. Q. Liu, and F. S. Zhang, "Recent progress in improving low-temperature stability of infrared thin-film interference filters," Opt. Express **13**(17), 6376–6380 (2005).
12. J. P. Borgogno, F. Flory, P. Roche, B. Schmitt, G. Albrand, E. Pelletier, and H. A. Macleod, "Refractive index and inhomogeneity of thin films," Appl. Opt. **23**(20), 3567–3570 (1984).
13. H. Rafla-Yuan, B. P. Hichwa, and T. H. Allen, "Noncontact method for measuring coefficient of linear thermal expansion of thin films," J. Vac. Sci. Technol. A **16**(5), 3119–3122 (1998).

#226657 - $15.00 USD Received 10 Nov 2014; revised 19 Dec 2014; accepted 22 Dec 2014; published 9 Jan 2015

14. K. Zhang, J. Seeley, R. Hunneman, and G. Hawkins, "Optical and semiconductor properties of lead telluride coatings," Proc. SPIE **1125**, 45–52 (1989).
15. C. Jacobs, "Dielectric square bandpass design," Appl. Opt. **20**(6), 1039–1042 (1981).
16. H. A. Macleod, *Thin-Film Optical Filters, Fourth Edition* (CRC Press, 2010).
17. H. Takashashi, "Temperature stability of thin-film narrow-bandpass filters produced by ion-assisted deposition," Appl. Opt. **34**(4), 667–675 (1995).
18. P. Baumeister, "Methods of altering the characteristics of a multilayer stack," J. Opt. Soc. Am. **52**(10), 1149–1152 (1962).
19. P. Klocek, *Handbook of Infrared Materials* (Marcel Dekker, Inc., 1991).
20. C.-H. Su, S. Feth, and S. L. Lehoczky, "Thermal expansion coefficient of ZnSe crystal between 17 and 1080°C by interferometry," Mater. Lett. **63**(17), 1475–1477 (2009).
21. Yu. I. Ravich, B. A. Efimova, and I. A. Smirnov, *Semiconducting Lead Chalcogenides* (Plenum Press, 1970).
22. Y.-H. Yen, L.-X. Zhu, W.-D. Zhang, F.-S. Zhang, and S.-Y. Wang, "Study of PbTe optical coatings," Appl. Opt. **23**(20), 3597–3601 (1984).
23. R. Dalven, "A review of the semiconductor properties of PbTe, PbSe, PbS and PbO," Infrared Phys. **9**(4), 141–184 (1969).
24. E. Palik, *Handbook of Optical Constants of Solids* (Acedemic Press, 1985).
25. R. A. Feldman, D. Horowitz, and R. M. Waxler, "Refractive properties of infrared window materials" *in Proceedings of Laser induced damage in optical materials*, (SPIE, 1977).
26. R. J. Harris, G. T. Johnston, G. A. Kepple, P. C. Krok, and H. Mukai, "Infrared thermooptic coefficient measurement of polycrystalline ZnSe, ZnS, CdTe, CaF(2), and BaF(2), single crystal KCI, and TI-20 glass," Appl. Opt. **16**(2), 436–438 (1977).
27. H. W. Icenogle, B. C. Platt, and W. L. Wolfe, "Refractive indexes and temperature coefficients of germanium and silicon," Appl. Opt. **15**(10), 2348–2351 (1976).
28. B. J. Frey, D. B. Leviton, and T. J. Madison, "Temperature-dependent refractive index of silicon and germanium," Proc. SPIE **6273**, 62732J (2006).
29. J. Thornton, "Absorption characteristics of low-resistivity germanium," Proc. SPIE **1112**, 94–98 (1989).
30. S.-H. Kim and C. K. Hwangbo, "Derivation of the center-wavelength shift of narrow-bandpass filters under temperature change," Opt. Express **12**(23), 5634–5639 (2004).
31. H. Takashashi, "Temperature stability of thin-film narrow-bandpass filters produced by ion-assisted deposition," Appl. Opt. **34**(4), 667–675 (1995).
32. G. J. Hawkins, R. E. Sherwood, B. M. Barrett, M. Wallace, H. J. B. Orr, K. Matthews, and S. Bisht, "High-performance infrared narrow-bandpass filters for the Indian National Satellite System meteorological instrument (INSAT-3D)," Appl. Opt. **47**(13), 2346–2356 (2008).
33. J. E. Murphy-Morris and S. W. Hinkal, "GOES Sounder Overview," Proc. SPIE **2812**, 174–181 (1996).
34. G. J. Hawkins, R. E. Sherwood, K. Djotni, P. M. Coppo, H. Höhnemann, and F. Belli, "Cooled infrared filters and dichroics for the Sea and Land Surface Temperature Radiometer," Appl. Opt. **52**(10), 2125–2135 (2013).
35. E. Ritter, "Properties of optical film materials," Appl. Opt. **20**(1), 21–25 (1981).
36. H. A. Macleod, "Microstructure of optical thin films," Proc. SPIE **325**, 21–28 (1982).

1. Introduction

It is a fundamental behavior of thin film narrow bandpass filters to exhibit large displacements of center wavelength with temperature. This attribute can be utilized for selective wavelength tuning of optical filters by controlling the temperature. However, it is generally a cause of concern to spectroscopists employing bandpass filters to discriminate between different molecular species with spectrally overlapping absorption signatures. Historically, infrared optical filters have been integrated in cooled and temperature stabilized detecting systems with working temperatures far-below the filter manufacturing conditions [1]. Therefore the filter designer has always needed to take wavelength shifts with temperature into consideration. However, current infrared technology is advancing toward the use of uncooled detectors [2–4] in which optical filters are increasingly embedded in infrared devices required to operate at room temperature and above in uncontrolled temperature environments [5]. In the absence of active temperature control, temperature-invariant optical bandpass filters are of increasing demand.

The inherent temperature shift in center wavelength of the narrow bandpass filter is governed by the temperature-dependency between paired optical properties of the multilayers, viz. the refractive index, index contrast and the physical thicknesses. These properties determine the integrated optical thickness of the bandpass coating, which defines the center wavelength. For most materials, the temperature coefficients of these paired materials are

#226657 - $15.00 USD Received 10 Nov 2014; revised 19 Dec 2014; accepted 22 Dec 2014; published 9 Jan 2015

positive, leading to optically thicker coating layers with increasing temperature, and subsequent displacement of center wavelength toward longer wavelength [6].

Lead Telluride (PbTe) is an exceptional semiconductor material that has been investigated extensively for mid-infrared optical filters for many years [7]. It is an extraordinary material for the following reasons [8]; the high refractive index when used with an appropriate low-index dielectric results in one of the highest practical known index contrasts (n_H/n_L) to achieve a prescribed spectral filtering function with the minimum number of layers and maximize throughput. The refractive index is one of the highest known of usable infrared layer materials with values of n ~5.5 at 300K rising to ~6.0 at 80K, (i.e. refractive index decreasing with increasing temperature), this contrast provides a high effective index (n^*), broadening the multilayer stop-band width and reducing spectral shift caused by inclined illumination [9]. Additionally for mid-infrared wavelengths PbTe provides continuous short-wavelength blocking by photo-absorption to ~3.2μm, further than all other commonly used evaporation materials due to the long-wave position of its semiconductor edge. Upon cooling the semiconductor absorption edge shifts to longer wavelengths (and hence shorter-wavelengths on heating) as a function of the anomalous increase in bandgap (PbTe ≅ + $4.2\text{x}10^{-4}$ eV K-1), common with all Pb-salts (PbTe, PbSe, PbS). For intrinsic PbTe at temperatures between 100K and 450K, the bandgap increases from ≅ 0.25 eV to ≅ 0.4 eV. This change produces a short-wavelength shift proportional to the inverse of the temperature moving from ~5.0 to 3.2 μm [10]. The optical dispersion properties of PbTe layer material are further strongly defined by the electronic carrier concentration, and departure from stoichiometry.

In this paper we pay specific attention to the negative dn/dT of PbTe as it presents unique possibilities to achieve temperature-invariant bandpass filter behavior. Figure 1 illustrates the principle of minimizing the net wavelength displacement with temperature using paired materials of PbTe and ZnSe. The blue and green curves show simulated bandpass displacements with wavelength due to the changes in thermal coefficient with increasing temperature applied singularly to each material. The red curves show the resultant net bandpass wavelength displacement across the 20-160 °C temperature range.

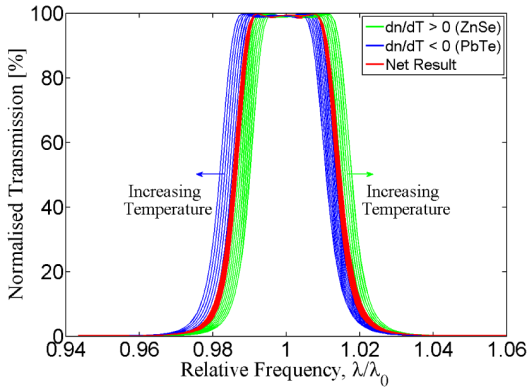

Fig. 1. Opposing optical layer properties resulting in wavelength immunity of PbTe/ZnSe narrow bandpass filter with temperature.

The application of temperature-invariant properties to infrared narrow bandpass filter design has been known for a number of decades, particularly with PbTe and ZnS paired materials discussed and demonstrated formerly for Fabry-Perot (FP) single-cavity and two-cavity Double Half-Wave (DHW) designs [8,11]. However, a systematic investigation of the design dependence of contemporary temperature-invariant three-cavity Triple Half-Wave (THW) filters has never been presented, and the rationale of temperature-invariant properties has remained undisclosed.

#226657 - $15.00 USD Received 10 Nov 2014; revised 19 Dec 2014; accepted 22 Dec 2014; published 9 Jan 2015

From a theoretical perspective, predicting the temperature and spectral response for a given thin film multilayer is straightforward, providing the material temperature coefficients of expansion and dispersion are well-known. However, this is generally not the case for thin films embedded in a multilayer operating in an environment above room temperature. Thin films generally possess different optical, thermal and mechanical properties compared to the isotropic bulk form [12,13]. Often bulk properties are insufficient to accurately predict the resulting thermal behavior of the thin film multilayer. Despite efforts in establishing these thin film opto-mechanical properties over many years [13,14], the knowledge of particular thermal expansion coefficients with temperature for any embedded thin film is still exceedingly sparse, if not unattainable. In Section 5 we review the available data for thermal expansion coefficients as well as the thermal dispersion coefficients of the two important layer materials for mid-infrared wavelengths, PbTe and ZnSe. Focusing solely on the optical and mechanical properties of these two materials reduces the complexity of this study as it limits the number of available design permutations, simplifying the characterization of the interdependence between multilayer design and temperature invariance. We are further directing this work towards elevated temperatures across the range 20-160 °C. Within this temperature range we expect temperature invariance to become of particular importance in future infrared detection. However, the design methods described in this paper are not constrained by these two materials or wavelength ranges, but applicable to other Pb salts (PbSe, PbS) in combination with other II-VI dielectric materials and temperatures.

2. Modelling procedure

The work reported here was divided into the following procedure; firstly to establish a knowledge database by conducting a literature survey to gather published knowledge of the refractive index temperature coefficient $\left(\frac{1}{n}\frac{dn}{dT}\right)$ (referred to as temperature dispersion coefficient, β_n), and the linear thermal expansion coefficient (α_L) for PbTe and ZnSe, in both thin film and bulk form. Secondly, to calculate the center wavelength temperature dependence $\left(\frac{1}{\lambda}\frac{d\lambda}{dT}\right)$ for various multilayer design arrangements of narrow bandpass filters based on published material properties. This is followed by predictions of temperature-dependence tested against measurements of thermal behavior from a repository of manufactured optical filters. This approach discloses whether the reported material properties can correctly predict the temperature response of manufactured filters, particularly, where some properties are in disagreement. Finally, to categorize multilayer designs with temperature-invariant behavior based on design bandwidth, cavity thickness order, and number of inter-cavity reflector layers. Here we present a simple model that successfully predicts the temperature response of manufactured bandpass filters.

3. Bandpass filter design

The narrow bandpass filters designed and manufactured for this investigation have comprised well-established triple half-wave (3-cavity) resonant multilayer designs using the high index contrast from the IV-VI lead telluride (PbTe, $n \approx 5.5$) semiconductor alternately paired with II-VI zinc selenide (ZnSe, $n \approx 2.4$) dielectric. This generic bandpass design approach has been fully described historically by Jacobs [15] with the advantage of deploying integral quarter-wave (λ/4) inter-cavity reflector stacks, use of multiple half-wave (λ/2, λ, 3λ/2 etc.) cavity thicknesses, and inclusion of antireflection matching periods between the equivalent bandpass core index and surrounding media. The nomenclature described in this paper assigns cavity thickness to either integral full-wave (λ) designation, comprising 2:2:2 to represent the half-wave order of the three cavities (i.e. 4:4:4 represents 3 cavities, each of λ thickness).

#226657 - $15.00 USD Received 10 Nov 2014; revised 19 Dec 2014; accepted 22 Dec 2014; published 9 Jan 2015

These generic bandpass filter designs have been deployed extensively throughout many former spaceflight filter missions, as described in Section 8, with advantages and compromise between spectral discrimination and manufacturability. As the energy grasp due to squareness of the bandpass shape improves with the number of cavities, the total number of index-matched paired layers and thickness of the multilayer also increases. In addition to this, the narrower the filter bandwidth is required to be, higher order thickness cavities are needed and larger number of inter-cavity layers necessary to match internal reflectivity from the cavities. As the bandwidth further reduces with increasing thickness, transmission losses due to absorption and multiple beaming rise sharply, which together with an increased sensitivity of bandpass shape to layer thickness errors, the perceived spectral advantage of improved bandpass shape diminishes with increased number of cavities. For mid-infrared wavelengths all of these factors mitigate against increasing designs beyond 3-cavities, often the result of limiting accuracy from *in situ* optical thickness monitoring during deposition.

4. Temperature-dependence theory

The center wavelength (λ_0) positioning of a bandpass filter is determined by the optical thicknesses of the coating layers. The optical thickness (δ) of a thin film layer is proportional to the product of the material properties; refractive index *n*, and physical thickness *l*, $(2\pi nl\cos\theta)/\lambda$. Since both of these properties change with temperature, λ_0 becomes temperature-dependent. However, the thin film materials comprising the multilayer stack will not change optical thickness equally or in the same direction, i.e. alternate layers become optically thinner with temperature, whilst the remaining layers optically thicken. Based on performance simulations through the multilayer characteristic matrix algorithm [10,16] (programmed through FTG FilmStar® proprietary thin film design software), we have determined that the contribution to the wavelength shift can be evaluated incrementally as discrete layers throughout the multilayer, with a design specific weighting factor assigning a sensitivity to individual layers opposing each other The center wavelength shift can thus be described by the following equation.

$$\frac{\mathrm{d}}{\mathrm{d}T}\frac{\lambda_0}{\lambda}=\sum_{m=1}^{q}s_m\frac{1}{\delta_m}\frac{\mathrm{d}\delta_m}{\mathrm{d}T}$$

where *m* is the layer number, *q* is the total number of layers, and s_m is a design specific layer sensitivity factor For a dual material filter this simplifies to;

$$\frac{\mathrm{d}}{\mathrm{d}T}\frac{\lambda_0}{\lambda}=s_L\frac{1}{\delta_L}\frac{\mathrm{d}\delta_L}{\mathrm{d}T}+s_H\frac{1}{\delta_H}\frac{\mathrm{d}\delta_H}{\mathrm{d}T} \tag{1}$$

where L and H are low and high refractive index materials respectively. The material weighting factors (S_L) and (S_H) are determined by the multilayer design. The temperature coefficient of the optical thickness relates to the temperature coefficients α_L and β_n;

$$\frac{1}{\delta}\frac{\mathrm{d}\delta}{\mathrm{d}T}=\frac{1}{nl}\frac{\mathrm{d}}{\mathrm{d}T}nl=\frac{1}{nl}\left(l\frac{\mathrm{d}n}{\mathrm{d}T}+n\frac{\mathrm{d}l}{\mathrm{d}T}\right)=\frac{1}{n}\frac{\mathrm{d}n}{\mathrm{d}T}+\frac{1}{l}\frac{\mathrm{d}l}{\mathrm{d}T}=\beta_n+\alpha_L$$

where we have recognized $\frac{1}{l}\frac{\mathrm{d}l}{\mathrm{d}T}$ as the linear thermal expansion coefficient, α_L, and $\frac{1}{n}\frac{\mathrm{d}n}{\mathrm{d}T}$ as the linear temperature dispersion coefficient β_n. Furthermore, we can now define the linear

#226657 - $15.00 USD Received 10 Nov 2014; revised 19 Dec 2014; accepted 22 Dec 2014; published 9 Jan 2015

thermo-optical expansion coefficient as $\gamma_L \equiv \frac{1}{\delta}\frac{\mathrm{d}\delta}{\mathrm{d}T} = \beta_n + \alpha_L$. Equation (1) can thus be substituted;

$$\frac{d}{dT}\frac{\lambda_0}{\lambda} = s_L\,\gamma^L + s_H\,\gamma^H = s_L\,\left(\beta_n^L + \alpha_L^L\right) + s_H\,\left(\beta_n^H + \alpha_L^H\right) \qquad (2)$$

For most conventional dielectric thin film materials, both β_n and α_L are positive values and thus λ_0 shifts toward longer wavelengths with increasing temperature. From Eq. (2) we see that in order to produce a filter with low temperature dependence, there are two different ways to proceed. One approach is to choose specific materials with minimal values of β_n and α_L. This approach is undertaken by Takashashi [17] where attention is directed to achieving bulk-like crystal properties of the thin film structure by ion-assisted deposition. A very different approach is to look for a special material having at least one negative temperature coefficient such that Eq. (2) by choice of multilayer design adds up to zero. This is the approach pursued by Seeley [8] and Li [11], as well as in this work. The enabling material is PbTe because of its negative change in refractive index ($dn/dT<0$) with increasing temperature. Li *et al* takes control of the negative coefficient by doping PbTe with Ge. Their focus is to target temperature-invariance to a specific temperature range. In this work we are not controlling temperature invariance, we are explaining and predicting how the multilayer design determines the temperature behavior of the bandpass filter. It is, however, our intention that the work presented here will contribute to gaining control over temperature invariance of optical filters in the future.

Equation (2) shows how the temperature response of the bandpass is determined by the temperature coefficients β_n and α_L of the constituent materials. The dependence on the multilayer design has been concealed in the sensitivity weighting factors, S_L and S_H which can be conveniently calculated by the help of multilayer design software. Mathematically demonstrated by Baumeister [18], the impact of a change in optical thickness of a single layer depends on the position inside the multilayer stack. The method was applied by Seeley [8] to determine; i) the cavity layer in a Fabry-Perot bandpass filter is significantly more sensitive to thickness changes than the surrounding layers, ii) a double half-wave cavity is twice as sensitive to thickness changes as a single half-wave cavity, and iii) the reflector layers adjacent to the cavity are three times more sensitive than the successive inter-cavity layers. According to these findings, the order of the filter should have major influence on the temperature response of the bandpass, as confirmed and demonstrated by the spectral measurement data presented in Section 8.

5. Optical material properties

The optical properties of thin films are well-known to deviate from the isotropic bulk material properties, often due to crystal morphology structure or film porosity resulting from reduced packing density (ρ), yet measurements of optical properties of thin films are usually made on exposed single layer films deposited on a substrate. Embedded thin films within a multilayer are likely to further possess optical properties between bulk and single film values, yet they are not easily measured and only derived by assumptions.

5.1 Linear thermal expansion coefficient (α_L)

The linear thermal expansion coefficient (α_L) is well-established for most bulk materials and can be found in reference literature handbook sources such as Klocek [19]. However, recently α_L for bulk ZnSe was measured using Fabry-Perot interferometry designed for elevated

#226657 - $15.00 USD Received 10 Nov 2014; revised 19 Dec 2014; accepted 22 Dec 2014; published 9 Jan 2015

temperatures (17-1080 °C) from which values of α_L were reported by Su *et al* [20] to be 35% below handbook values at room temperature. The authors do not comment on this deviation. Rafla-Yuan *et al* [14] measured ZnSe α_L for 1.7 μm thick single thin film by ellipsometry from which values significantly larger than bulk properties were reported, as illustrated in Fig. 2. The authors explain the large discrepancy from bulk as a result of film packing density, stress, and thermal expansion mismatch between film and substrate. As their reported values are measured on single exposed thin films, they cannot be expected to apply for the embedded thin film in an interference multilayer. In fact, the thin film values from Rafla-Yuan vary so radically with temperature that they can be instantly excluded from our study due to the corresponding center wavelength displacement being considerably larger than observed in measurements. Further, the increase with temperature would mean that the displacement rate, $\Delta\lambda_0$/°C should increase with temperature, which is also not observed. This maintains the continued use of existing bulk ZnSe literature data.

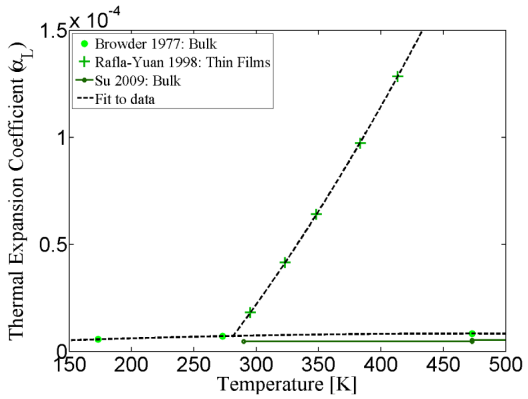

Fig. 2. Comparison of reported thermal expansion of thin film and bulk values of ZnSe

Linear thermal expansion data for thin film PbTe is not reported in the literature, but is available for bulk PbTe. Ravich *et al* [21] reports the thermal expansion coefficient across a 25-320 K temperature range, with a stable plateau value above 200 K of 2.0 x10^{-5} K^{-1} with increasing temperature. Figure 3 shows the bulk α_L values in the multilayer simulations for both ZnSe and PbTe.

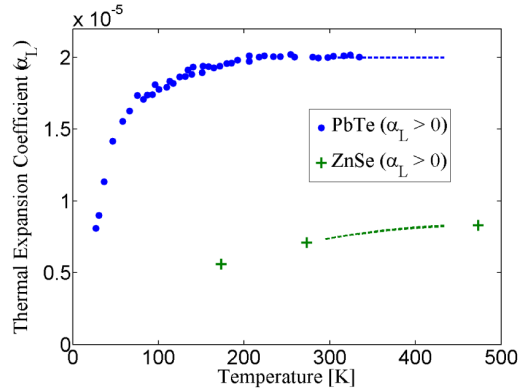

Fig. 3. Thermal expansion coefficients of bulk material for PbTe and ZnSe. (Dashed lines indicate the values deployed in the simulations).

#226657 - $15.00 USD Received 10 Nov 2014; revised 19 Dec 2014; accepted 22 Dec 2014; published 9 Jan 2015

5.2 Optical dispersion temperature coefficient (β_n)

The exact refractive index of PbTe is known to depend on the properties of evaporable material composition [22]. Zhang *et al* [14] characterized the refractive index of tellurium-enriched PbTe thin films with a dispersive shape showing similar generic properties to PbTe bulk material. The refractive index was determined for incremental temperatures between 45K and 463K across the complete inter-band transparent spectral range, (i.e. between electronic and multiphonon lattice absorption edges). The refractive index derived from spectral measurement is slightly lower than handbook bulk values [23,24] at corresponding temperatures as shown in Fig. 4.

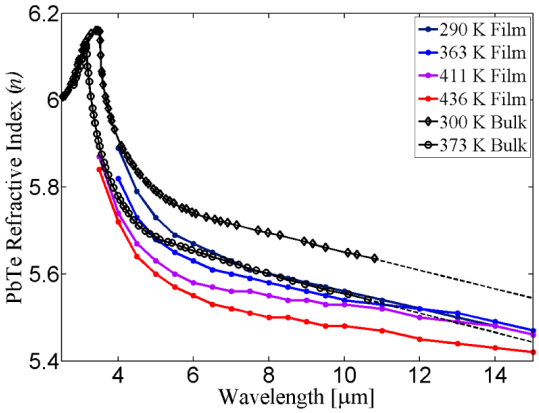

Fig. 4. Overlay of dispersion curves for bulk and thin film PbTe material (17-163K).

The temperature derivative (i.e. the temperature dispersion coefficient, $\beta_n = \frac{1}{n}\frac{\mathrm{d}n}{\mathrm{d}T}$), however shows a significant difference between thin film coating and bulk index as shown in Fig. 5. The bulk values were calculated by interpolation between the two fitted dispersion curves at 300 K and 373 K in Fig. 4. Interpolation between two values reveals no information about a possible temperature-dependence of β_n^{PbTe}. Thus a constant value is assumed and used in the simulation across the 20-160 °C temperature range. For the thin film PbTe material there are four different temperatures in our range of interest. However, the thin film data in Fig. 4 shows a very non-linear temperature behavior which is not in agreement with our measurements on manufactured filters as these generally exhibit smooth wavelength displacements with temperature. The stated uncertainty of the thin film data is 0.01 to 0.05 which may contribute significantly to the apparent nonlinear behavior. Instead we have chosen to use only the data sets at 290 K and 436 K which are separated by values greater than the uncertainty. As in the bulk case, two points per wavelength remain from which we derive a temperature independent value for thin film β_n^{PbTe}. This value is significantly smaller than the corresponding bulk value and leads to a very different prediction of the center wavelength shift. Figure 5 further shows a mean value between bulk and thin film as this turns out to be in best agreement with the measured spectral data, which we shall discuss in Section 8.

#226657 - $15.00 USD Received 10 Nov 2014; revised 19 Dec 2014; accepted 22 Dec 2014; published 9 Jan 2015

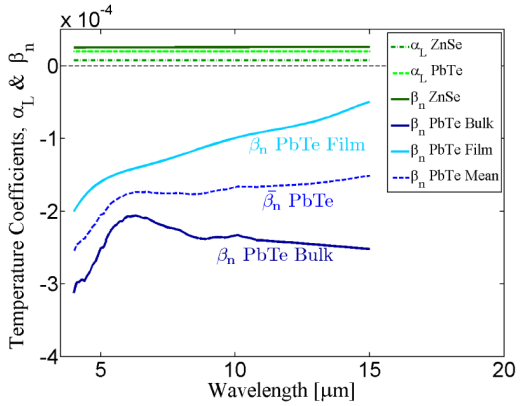

Fig. 5. Dispersion temperature coefficient ($\boldsymbol{\beta_n}$) and linear thermal expansion coefficient ($\boldsymbol{\alpha_L}$) of PbTe and ZnSe.

For ZnSe material we were unable to find any published data on thin film properties so also here it was necessary to use bulk properties. Feldman *et al* [25] measured *dn*/*dT* for a number of bulk infrared materials, including ZnSe, for a range of temperatures and a few different wavelengths. The values found for ZnSe in this work are 15% larger than corresponding measurements reported by Harris *et al* [26] earlier in the same year. This deviation made the authors repeat the measurement using a different method from which they obtained comparable results to their first measurements. Furthermore, Feldman *et al* generally found good agreement with other studies for their measurements of other materials. Based on this we choose to use the Feldman results from [25] for β_n^{ZnSe}, from which it is noted that the wavelength-dependence of the ZnSe temperature dispersion coefficient is very small compared with PbTe.

The results in Fig. 5 summarizes our review of the optical properties for PbTe and ZnSe, from which constants are presented in Table 1. For α_L^{ZnSe}, α_L^{PbTe}, and β_n^{ZnSe} we have not located any useful reference data in thin film form, thus have applied bulk properties to the model. Conversely, for β_n^{PbTe} we have acquired both thin film and bulk data. From the results illustrated in Fig. 5 together with interpretation of Eq. (2), it is evident that owing to the magnitude of β_n^{PbTe}, this temperature coefficient contributes the largest impact on center wavelength displacement.

Table 1. Results of review of mid-infrared optical properties of ZnSe and PbTe (20 - 160 °C)

Coefficient	Bulk	Thin film	Data Origin
α_L^{ZnSe}	+ 0.77 x 10^{-5} K^{-1}	-	[20]
α_L^{PbTe}	+ 2.0 x 10^{-5} K^{-1}	-	[22]
β_n^{ZnSe}	+ 2.6 x 10^{-5} K^{-1}	-	[26]
β_n^{PbTe} (at 10 μm)	- 23 x 10^{-5} K^{-1} *	–9.9x10^{-5} K^{-1} *	[24] [15]

6. Bandpass simulations

Using the derived temperature coefficients described above, calculations to simulate the influence of elevated temperature on various bandpass designs, wavelengths, and cavity thicknesses were performed through conventional multilayer calculation theory. Example of simulation results for a generic multilayer design with different cavity thicknesses are shown in Fig. 6. This common multilayer bandpass design located at 4 and 10 μm comprises

#226657 - $15.00 USD Received 10 Nov 2014; revised 19 Dec 2014; accepted 22 Dec 2014; published 9 Jan 2015

incremental half-wave thickness for the three cavities. The simulations shown are performed using bulk properties for α_L^{ZnSe}, β_n^{ZnSe} & α_L^{PbTe} and with a mean coefficient between bulk and thin film properties for β_n^{PbTe}.

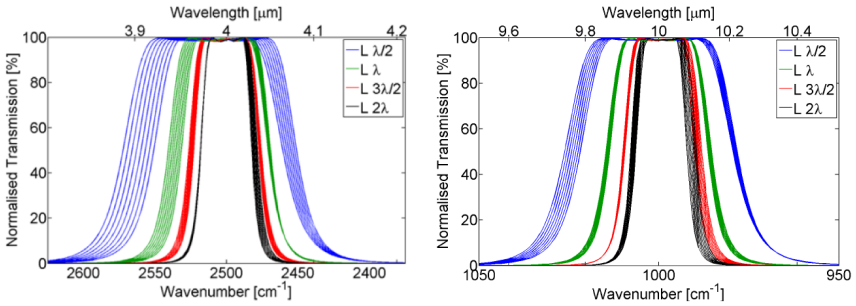

Fig. 6. Simulated temperature response of four different thickness-order L-cavity ZnSe/PbTe bandpass filters at 4 and 10 μm. Each color covers the range 20-160°C in steps of 20°C

The bandpass simulations in Fig. 6 reveal an asymmetry of edge positions with temperature wavelength shift. This asymmetric displacement is the result of bandwidth broadening that occurs simultaneously with opposing index coefficients. As the bandwidth is determined by the index contrast between the paired layer materials (n_H/n_L), the opposing temperature coefficients maintain wavelength stability, however the reduced index contrast broadens the bandwidth ($\Delta\lambda/\lambda_0$). As a result, the opposing edges are displaced differently. For the purpose of discriminating between absorption lines, the edges are actually of greater interest than the center wavelength displacement. From the perspective of center wavelength displacement the 3λ/2 cavity thickness is very good, but in mid-infrared spectroscopy the 2λ or even λ-cavity filters might be preferred because of the stable edges on the short-wave and long-wave side, respectively. However, for the purpose of this paper we will continue to discuss center wavelength displacement to comply with existing literature on temperature invariance. Yet, since edge-wavelength shift is of equal importance, this information together with center wavelength shifts obtained from the repository of manufactured bandpass filters is included in the summarized results in Table 3. For each design wavelength and cavity order, the center wavelength shift with temperature is determined. The resulting values are illustrated as circles in Fig. 7 along with the calculations from Eq. (2) using the weighting factors given in Table 2. Evidently, using Eq. (2), the optical properties, and the design dependent weighting factors, temperature-invariance can be predicted without need of performing any multilayer calculations.

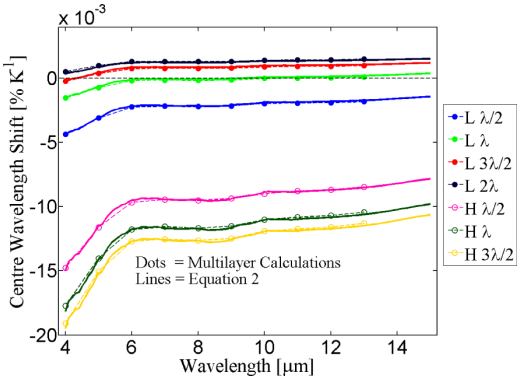

Fig. 7. Overlay of simulated center wavelength displacement (circles), and displacement predicted from Eq. (2).

#226657 - $15.00 USD Received 10 Nov 2014; revised 19 Dec 2014; accepted 22 Dec 2014; published 9 Jan 2015

Table 2. Weight factors for Eq. (2).

Sensitivity factors	L –Cavity λ/2	L –Cavity λ	L –Cavity 3λ/2	L –Cavity 2λ	H –Cavity λ/2	H –Cavity λ	H – Cavity 3λ/2
S_L [%]	71	82	87	89	32	20	15
S_H [%]	29	18	13	11	68	80	85

Results from Fig. 7 indicate that achievement of wavelength invariance at elevated temperature across the 6-13 µm range using ZnSe and PbTe materials, is best performed with a cavity thickness of λ. This however subsequently infers compromise between optimal temperature-invariance and desired bandwidth. At wavelengths below 6 µm higher orders are necessary to achieve wavelength-invariance.

7. Substrate temperature influence

Thin film dielectric multilayers deposited on germanium are perhaps the most extensively used material combination in the context of cooled mid-infrared filtering applications. It exhibits low absorption across the 2-12 µm wavelength range with a bandgap of ~0.67 eV at ambient temperature. At elevated temperatures however, standard optical grade material is known to be subject to substantial absorption losses throughout the infrared waveband due to the increased number of thermally generated free carrier holes. Germanium is hence generally not suited as a substrate for high temperature applications. The temperature-dependent refractive index of germanium has been reported by Icenogle *et al* [27] and Frey *et al* [28] for operation in cooled temperature environments. Spectral measurements of many infrared substrate materials at elevated temperatures are however sparse. Thornton [29] measured Ge transmission in increments up to 150 °C for two differing resistivity samples across the 7-15 µm range. The II-VI dielectrics, however, remain transparent for temperatures up to at least 200 °C. Figure 8 shows temperature measurements of uncoated optical windows of ZnSe, ZnS and Ge for temperatures between 20 – 200 °C.

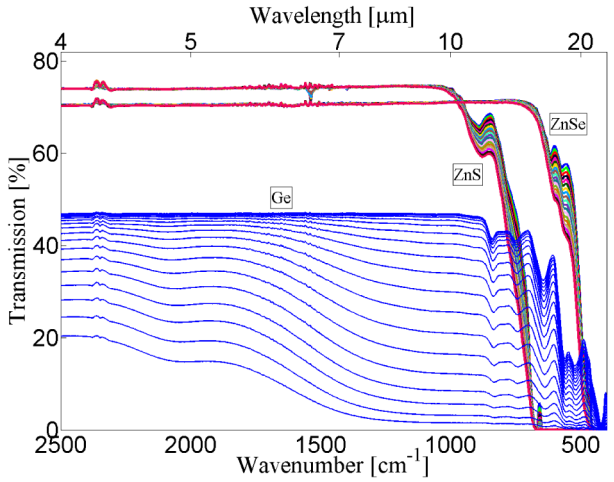

Fig. 8. Measured transmission of 4 mm thick ZnS, ZnSe and Ge uncoated substrate materials at temperatures from 20 °C to 200 °C at 20 °C increments.

A substantial number of the spectral measurements presented in this paper are deposited on germanium, particularly as the filters were designed for cryogenic operation. This, however, does not compromise the validity of the elevated temperature-invariance comparison. We have compared filters of similar multilayer design deposited on different substrates, as shown in Fig. 9, from which the substrate material is observed to influence wavelength shift to a lesser degree than the variations stemming from uncertainties in

#226657 - $15.00 USD Received 10 Nov 2014; revised 19 Dec 2014; accepted 22 Dec 2014; published 9 Jan 2015

manufacture. The two filters at 4 μm were further fabricated within the same deposition, which meant that one of the filters had to suffer from poor optical matching, distorting the bandpass shape, but showing no influence to the temperature behavior. From this we conclude that both substrate material as well as optical matching is inconsequential to the temperature variations of the bandpass filter. This is in agreement with theoretical findings in [30].Whilst we consider this a significant and important conclusion, it might not be transferable to other material arrangements and wavelengths, since in [31] thermal expansion of the substrate is found to have great influence on the center wavelength temperature stability of TiO_2/SiO_2 bandpass filters. In Section 9 we further investigate the influence of layer thickness errors which show that this also is without significant impact on the temperature-dependence.

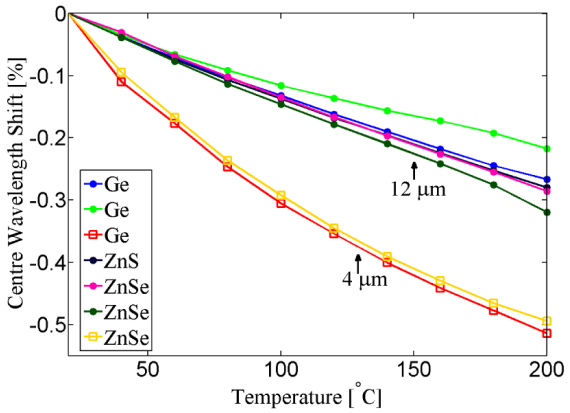

Fig. 9. Center wavelength shift for several filters of similar bandpass design deposited on differing substrate materials at wavelengths of 4 μm and 12 μm.

8. Comparison with manufactured filters

In order to validate the accuracy of predicted results from the temperature-invariance model presented in Fig. 7, spectral measurements at incremental temperature were performed on a historic repository of narrow bandpass filters originating from Earth observing spaceflight radiometer instruments. This library of filters represents a wide cross-section of generic multilayer bandpass design types and wavelengths, comprising both L- and H-spaced integral thickness cavities, differing cavity thickness orders, operating temperature requirements and center wavelength positioning.

Narrow bandpass filters from two missions; the NASA Aura mission High Resolution Dynamics Limb Sounder (HIRDLS) [1] and Indian Space Research Organization (ISRO) INSAT-3D [32] atmospheric sounder instruments comprised a wide range of differing bandpass designs containing 3-cavity triple half-wave (THW) low-index (L) cavity layers with differing thickness orders using alternate ZnSe and PbTe layers deposited on Germanium (Ge) optical substrates. The HIRDLS instrument bandpass filters were deployed in the focal plane detector array of this limb-viewing infrared radiometer which was designed for high resolution monitoring of global stratospheric and mesospheric temperatures and chemical species in the atmosphere at wavelengths between 6 and 18 μm. These filters were designed for high precision of spectral placement (typically, $\Delta\lambda_0 = \pm 1$ cm^{-1}), and located at an intermediate focus of the instrument, thermostatically controlled at 301K to provide the waveband definition through a low converging (*f*/5.5-*f*/7) conical illumination.

Bandpass filters manufactured for the INSAT-3D sounder instrument were developed for high resolution monitoring of temperature and trace species in the atmospheric region between the troposphere and stratosphere over the Bay of Bengal and Arabian Sea. These filters comprised precision L-cavity narrow bandpass designs between 1% and 6% full width half max (FWHM) to isolate wavelengths over the long-wave (LWIR 12-15 μm) and mid-

#226657 - $15.00 USD Received 10 Nov 2014; revised 19 Dec 2014; accepted 22 Dec 2014; published 9 Jan 2015

wave (MWIR 6.5-11 μm) spectral regions. These filters were designed to operate at a temperature of 210K in a collimated *f*/10 parallel beam. Similar wavebands of the INSAT-3D sounder are also deployed on the NOAA GOES geostationary satellite [33].

A third mission, comprising the Sea and Land Surface Temperature Radiometer (SLSTR**)** [34] is an instrument designed to provide climate data of global sea and land temperatures within the framework of the ESA Copernicus programme for the European polar orbiting Sentinel-3 satellite mission. The design of mid-IR narrow bandpass filters at 10.85 and 12.0 μm in this case employed high-index (H) cavity layer material to minimize wavelength shifts due to conical illumination (*f*/1.46) at the focal plane of the instrument. As one of the highest known refractive index materials, the use of PbTe cavity material provides a high effective index (*n**) to reduce sensitivity to non-parallel illumination ($d\lambda/d\theta$), however PbTe also possesses a large temperature coefficient ($d\lambda/dT$) when deployed in cavities, negating any temperature-invariant properties. This filter set provides a suitable cross-reference of an alternative generic bandpass design type to validate the wavelength displacement properties of the presented invariance model.

Further L-cavity narrow bandpass filters with temperature-invariant properties were manufactured at wavelengths of 4.3, 7.7, 10.3 and 12.1 μm deposited on CVD Zinc Sulphide (Multispectral ZnS, Cleartran®), Zinc Selenide (ZnSe) and Germanium (Ge) optical substrate materials. These items were manufactured with center wavelengths and spectral properties for industrial gas monitoring.

Table 3. Analysis of mean temperature shift from a repository of manufactured bandpass filters (20–120 °C) (Deposited on Ge, ZnSe and ZnS optical substrates).

Generic 3-Cavity Design	Bandpass Center at 20 °C (λ_0, μm)	Bandwidth (FWHM,%)	SW Edge Thermal Shift ($10^{-3\%}$ K^{-1})	Center λ_0 Thermal Shift ($10^{-3\%}$ K^{-1})	σ* for Center λ_0 Thermal Shift ($10^{-3\%}$ K^{-1})	LW Edge Thermal Shift ($10^{-3\%}$ K^{-1})
H - 2:2:2	10.47	10.49	–10.51	–8.87	-	–7.04
H - 2:2:2	11.77	8.42	–9.55	–8.35	-	–7.05
L - 2:2:2	4.3	3.8	–4.6	–3.2	0.5	–1.7
L - 2:2:2	11.4	4.5	–3.0	–1.9	-	–0.6
L - 2:2:2	12.1	4.4	–2.3	–1.6	0.2	–0.9
L - 2:2:2	15.8	4.3	–2.7	–1.8	0.0	–0.8
L - 2:2:2	17.5	3.9	–2.5	–1.7	-	–0.8
L - 2:4:2	7.3	3.2	–1.4	–0.4	0.6	0.7
L - 4:2:2	6.9	3.9	–2.2	–1.3	0.2	–0.3
L - 4:4:4	4.3	2.6	–1.8	–0.9	0.2	0.1
L - 4:4:4	7.6	2.8	–0.8	–0.1	0.2	0.5
L - 4:4:4	10.3	2.6	–0.5	–0.0	0.1	0.5
L - 4:4:4	12.1	2.8	–0.8	–0.5	0.6	–0.1
L - 4:4:4	16.4	2.9	–0.3	0.3	-	0.8
L - 4:6:4	13.6	2.3	0.4	0.8	0.1	1.2
L - 4:6:6	14.7	2.2	0.5	1.0	-	1.4
L - 6:4:6	9.7	2.4	0.0	0.6	-	1.2
L – 6:6:6	4.2	1.9	–0.6	0.1	0.1	0.8
L – 6:6:6	12.0	2.0	0.5	0.9	0.0	1.3
L – 6:6:6	14.2	2.0	0.8	1.1	0.3	1.5
L - 6:8:8	8.3	1.7	1.1	1.5	-	2.0

*Sample Standard deviation. Range of sample quantities are between 2 and 5 filter elements.

A total of 45 manufactured narrow bandpass 3-cavity filters with ZnSe and PbTe layer materials were systematically measured across a range of elevated temperatures between 20 and 200 °C at 20 °C intervals. Figure 10 shows a representative center wavelength displacement with temperature at 4 and 12 μm. The shift is observed to deviate from linearity

#226657 - $15.00 USD Received 10 Nov 2014; revised 19 Dec 2014; accepted 22 Dec 2014; published 9 Jan 2015

with a tendency to reduce at the higher temperatures. The effects of non-linear wavelength shift at the higher temperatures has implied an irregular material property from which our data analysis was constrained to a 100 °C range between 20 °C and 120 °C. By comparison, simulations predict a linear shift with temperature as there is no temperature-dependence in the coefficients. Based on this truncated measurement data, we determined the center wavelength and 50% FWHM edge shifts for all the filters measured. The obtained shift values are given in Table 3 and shown in Fig. 10 as a function of cavity order, viz. the one property with the most significant effect on temperature invariance. Spectral measurements and visual inspection from the elevated temperature excursions showed no evidence of either residual thermal hysteresis or mechanical damage, with exception of a single filter which experienced environmental deterioration at 200 °C. All filters showed a linear or slowly declining displacement with temperature up to 120 °C.

The influence of deposition temperature has not been specifically evaluated in this work, but is further known to affect both the sticking coefficient [35] and environmental properties due to the influence on packing density and microstructural morphology of the condensed films [36].

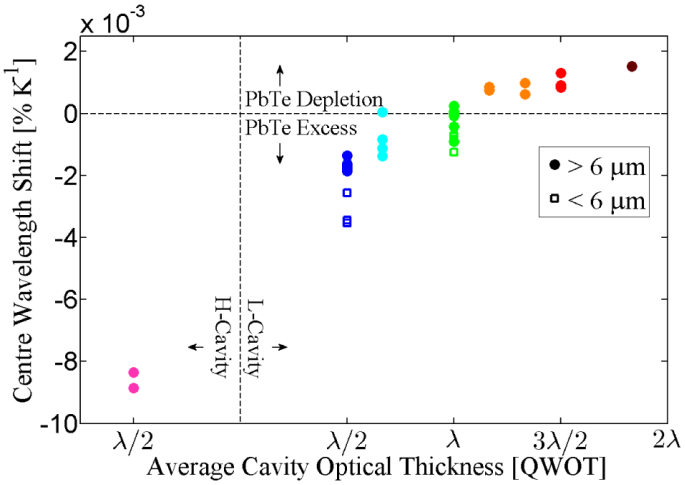

Fig. 10. Center wavelength shift of manufactured filters with cavity thickness and temperature (20-120 °C).

In Fig. 10 there is a clear relationship between cavity order and center wavelength displacement. The positive wavelength shift of high L-cavity orders represents a deficiency of PbTe material. Reducing the order, and associated increasing filter bandwidth, reduces the relative amount of ZnSe in the multilayer and the positive wavelength shift is decreased accordingly, continuing until the balance is opposed from which the filters begin to shift to shorter wavelengths with increasing temperature. For an H-cavity filter, the excess of PbTe leads to a negative center wavelength displacement worse than the typical positive center wavelength displacement of 0.005 [% K^{-1}] described in reference literature sources [16]. With the appropriate material balance several infrared filters with center wavelength displacements below 0.00015 [% K^{-1}] were realized over a wide wavelength range. Some examples of these are shown in Fig. 11, where the measured transmission profiles are illustrated for filter temperatures between 20 and 200 °C in steps of 20 °C.

#226657 - $15.00 USD Received 10 Nov 2014; revised 19 Dec 2014; accepted 22 Dec 2014; published 9 Jan 2015

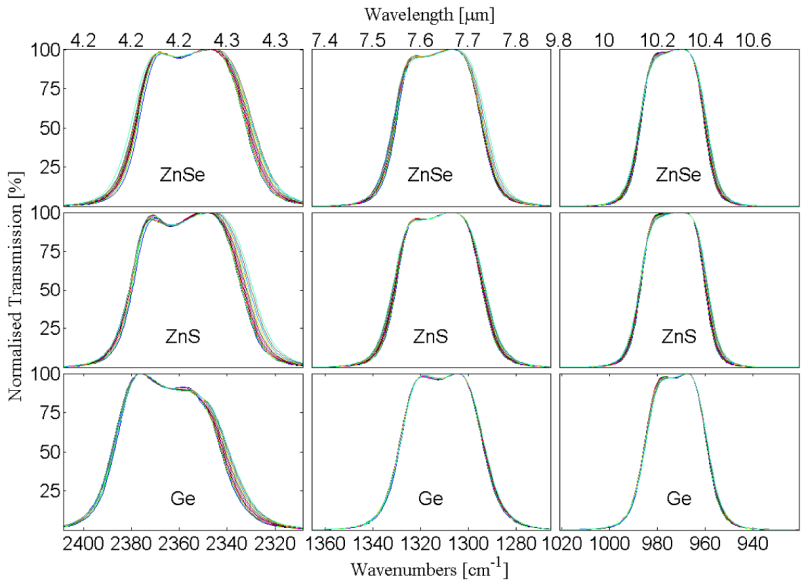

Fig. 11. Example normalized transmission measurements of 3-cavity bandpass filters at 4.2 μm, 7.6 and 10.3 μm showing temperature invariance in the range 20 - 200 °C.

In Fig. 12 the measured bandpass center shifts for all 45 filters are shown as a function of wavelength, together with the theoretically predicted temperature response based on bulk values of α_L and β_n for ZnSe, and for PbTe using bulk values of α_L and an average between bulk and thin film values for β_n. Whilst the true value for the embedded films are expected to be somewhere between the values of single thin film and bulk, there is no reason to assume that the value is exactly the average. However, the simple average leads to a remarkably good correspondence with experimental data. Using either thin film data or bulk data for PbTe (β_n) demonstrated, on the contrary, very poor agreement with the measured shifts (not shown). Figure 12 shows that within the confines of paired PbTe/ZnSe 3-cavity narrow bandpass filter materials, an optimal temperature-invariance can be achieved, but is restricted to a specific bandwidth. To gain more degrees of freedom and enabling temperature-invariant bandpass behavior at intermediate bandwidths, a third material might be included.

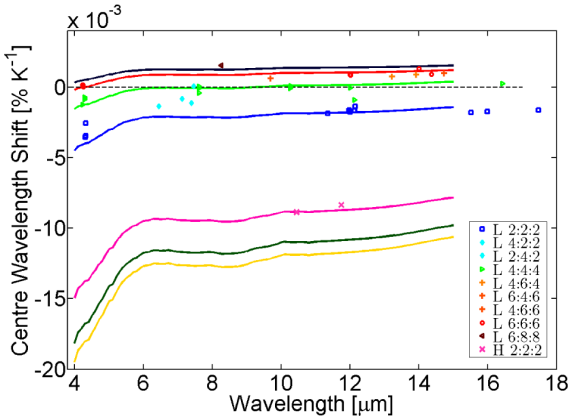

Fig. 12. Predicted center wavelength shift (lines) compared with measured wavelength shifts (symbols).

#226657 - $15.00 USD Received 10 Nov 2014; revised 19 Dec 2014; accepted 22 Dec 2014; published 9 Jan 2015

9. Layer thickness errors

Thickness errors of thin film layers are of key concern to the bandpass manufacture, particularly for matched accuracy of the cavities, as they compromise perfection of band shape, bandwidth and wavelength positioning. The fabricated filters to which we compare our simulations, inevitably all contain some degree of thickness error. We have investigated the degree to which such errors affect the wavelength displacement with temperature. Figure 13 shows simulated temperature variations of the bandpass transmission profile of a PbTe/ZnSe bandpass filter without thickness error, together with the same multilayer design but containing thickness errors introduced to the center cavity, particularly as this is known to be a dominating layer which is most sensitive to deviations [8]. No consequence was found of thickness errors on the wavelength displacement with temperature, even for gross thickness errors added to the most sensitive cavity layers. It should be noted, that introducing errors to adjacent cavities or inter-cavity reflector layers lead to the same conclusion. This analysis verifies that our simulations may be compared with fabricated filters without concerns regarding the influence of thickness errors. In fact, the results further allow us to make the general conclusion that thickness perfection plays no role in influencing temperature-invariance.

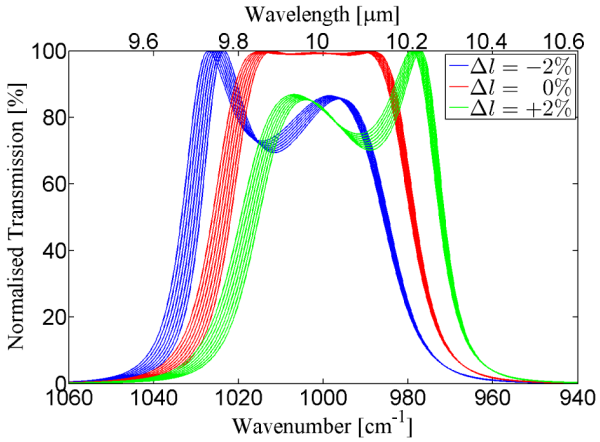

Fig. 13. Temperature variations of a multilayer design without thickness errors, and with gross thickness error applied to the center cavity of ± 2%.

10. Conclusions

A systematic investigation into the interdependence between multilayer bandpass design, optical materials, and wavelength properties of narrow bandpass filters has been presented. It has been shown that the temperature coefficients of bulk material are insufficient in predicting temperature wavelength dependence of narrow PbTe/ZnSe based bandpass filters. A set of material temperature properties that are able to describe the temperature wavelength behavior of PbTe/ZnSe narrow bandpass filters in good agreement with a historic repository of narrow bandpass filters were given for the temperature range 20-120 °C and the wavelength range 4-15 μm. It was shown experimentally that the cavity order determines the temperature wavelength behavior, implying that temperature invariance for a two-material filter is restricted to certain bandwidths. Mixed cavity orders can be used to tune the wavelength displacement to a desired value. Temperature measurements of different substrate temperature behavior at elevated temperature has been presented and it was shown that substrate material had insignificant influence on temperature invariance of these specific narrow band filters, even with increasing substrate absorption and optically mismatched thin film design. Finally,

#226657 - $15.00 USD Received 10 Nov 2014; revised 19 Dec 2014; accepted 22 Dec 2014; published 9 Jan 2015

it was shown that layer thickness errors neither contribute nor compromise the temperature-invariance sensitivity of the narrow bandpass filter design.

Acknowledgments

The authors thank colleagues at Schlumberger Cambridge Research for discussions and grateful support under contract reference QU-RDU-01274-C, together with the loan of a spectrometer accessory for high-temperature measurements. Thomine Stolberg-Rohr is a visiting industrial PhD student from Danfoss IXA A/S and her work is supported by the Danish Agency of Science, Technology and Innovation (DASTI). Thanks also to Richard Sherwood and Karim Djotni at the University of Reading for their assistance with spectral measurements and thin film depositions, which is gratefully acknowledged.

#226657 - $15.00 USD Received 10 Nov 2014; revised 19 Dec 2014; accepted 22 Dec 2014; published 9 Jan 2015